DØ Note 4336-Conf - FINAL Version, 2/25/04

Search for Large Extra Dimensions in the Dielectron and Diphoton Channels with 200 pb^{-1} of Run II Data

The DØ Collaboration
URL: http://www-d0.fnal.gov

(Dated: February 25, 2004)

We report preliminary results on a search for large spatial extra dimensions in the dielectron and diphoton channels using ~ 200 pb^{-1} of data collected by the DØ Experiment at the Fermilab Tevatron in 2002-2003 (Run II). We set a new lower 95% CL limit on the fundamental Planck scale of 1.36 TeV (in the GRW convention), significantly exceeding the limits obtained in Run I. Combined with the published Run I result, this correspond to a lower limit of 1.43 TeV, which is the most stringent limit on Large Extra Dimensions to date.

Preliminary Results for Winter 2004 Conferences

I. INTRODUCTION

That we live in a three-dimensional space may seem to be a well-known fact; however it lacks rigorous experimental proof. Recent advances in string theory suggest that there might exist hidden dimensions in space of a finite size R beyond the three we sense daily. More recently, in 1998, an attractive realization of the above idea has been proposed by Arkani-Hamed, Dimopoulos, and Dvali [1] (ADD). In their formulation, the standard model (SM) particles are confined to a 3-dimensional membrane (D3-brane), as expected in the string theory, and SM gauge interactions are therefore restricted to this brane. At the same time, gravity is allowed to propagate in the n extra spatial dimensions, which explains its apparent weakness. Fundamentally, gravity is as strong as other gauge forces, but this becomes apparent only for a $(3+n)$-dimnesional observer. The apparent Planck scale of $M_{\rm Pl} = 1/\sqrt{G_N} \sim 10^{19}$ TeV $\gg M_{\rm EW} \sim 1$ TeV merely reflects its volume supression due to the dilution in extra space.

Assuming that the fundamental, $(3+n)$-dimensional Planck scale, M_S, is in the TeV range, suggests for $n = 1$ a very large $R \sim 10^8$ km (of the size of our solar system), which is ruled out by the known $1/r^2$ dependence of the gravitational force at large distances. However, for $n \geq 2$ the expected R is less than 1 mm, and therefore does not contradict existing gravitational experiments. For instance, for $n = 2$ we have $R \sim 1$ mm. For larger n, compactification radius drops as a power law (*e.g.*, ~ 3 nm for $n = 3$). Thus $n = 2$ is the minimum number of these, *large* extra dimensions (ED).

While tabletop gravity experiments and astrophysical constraints have begun to produce tight limits on the fundamental Planck scale for the case of 2 extra dimensions, for any $n \geq 3$ they are easily eluded, which leaves high-energy colliders as the only sensitive probe for $n \geq 3$. Current best lower limits on the fundamental Planck scale for $n \geq 3$ come from LEP and the Tevatron Run I; they are ≈ 1 TeV. Limits from HERA are some 20% less restrictive.

The two main ways of probing large extra dimensions at colliders is to look for the production of a real graviton recoiling against a gauge boson or a quark in a high-energy interaction (which results in a monojet, or monophoton signature) and to look at the effects of virtual gravitons in the fermion or boson pair production. Both types of studies were performed at LEP and at the Tevatron, with DØ having pioneered search for large extra dimensions at hadron colliders by analyzing dielectron and diphoton final states [2] and more recently from the complementary monojet channel [3].

II. METHOD

In this paper, we focus on new results in the dielectron and diphoton channels, obtained using ~ 200 pb^{-1} of data collected by DØ in Run II in 2002–2003.

The effects of ED are parameterized via a single variable $\eta_G = \mathcal{F}/M_S^4$, where $\mathcal{F}$ is a dimensionless parameter of order unity, reflecting the dependence of virtual $G_{\rm KK}$ exchange on the number of extra dimensions. Different formalisms use different definitions for $\mathcal{F}$:

$$\mathcal{F} = 1, \text{ (GRW [4])}; \tag{1}$$

$$\mathcal{F} = \begin{cases} \log\left(\frac{M_S^2}{M^2}\right), & n = 2 \\ \frac{2}{n-2}, & n > 2 \end{cases}, \text{ (HLZ [5])}; \tag{2}$$

$$\mathcal{F} = \frac{2\lambda}{\pi} = \pm\frac{2}{\pi}, \text{ (Hewett [6])}. \tag{3}$$

In both the GRW and HLZ models, the sign of interference between the SM and the effects of large ED is shown to be positive. In a more emprical, Hewett's model, neither the sign of the interference, nor the magnitude of the amplitude is fixed. The unknown effects of gravity are parameterized via a parameter λ of order one, which can be either positive or negative. We will use $\lambda = \pm 1$ to translate the limits on η_G into the limits on M_S in Hewett's formalism. Note that only within the HLZ formalism $\mathcal{F}$ depends explicitly on n. The parameter η_G has dimensions of TeV^{-4} with M_S in units of TeV, and describes the strength of gravity in the presence of LED. While the physics meaning of scale M_S is an ultraviolet cutoff of a divergent sum over the winding modes of graviton in extra dimensions (Kaluza-Klein graviton tower), it is expected to be closely related to the fundamental Planck scale, as the latter gives a natural cutoff to this sum.

In this analysis we follow the prescription of Ref. [8] (also followed in the Run I DØ publication [2]) and analyze the dilepton or diphoton data in the plane of two variables that completely determine the leading order (LO) $2 \to 2$ scattering: the invariant mass of the dilepton or diphoton pair, and the cosine of the scattering angle in the center-of-mass (c.o.m.) frame, $\cos\theta^*$. This choice of variables yields optimum sensitivity to the contributions from extra dimensions [8].

To minimize the efficiency loss due to photon conversion and imperfect tracking, we combine the dielectron and diphoton channels, and in what follows refer to "diEM" objects. Consequently, we imply $|\cos\theta^*|$ instead of signed $\cos\theta^*$, whenever we refer to $\cos\theta^*$.

The cross section in the presence of large ED is given by [4–6]:

$$\frac{d^2\sigma}{dMd\cos\theta^*} = f_{\rm SM} + f_{\rm int}\eta_G + f_{\rm KK}\eta_G^2, \quad (4)$$

where $f_{\rm SM}$, $f_{\rm int}$, and $f_{\rm KK}$ are functions of $(M, \cos\theta^*)$ and denote the SM, interference, and $G_{\rm KK}$ terms.

III. MONTE CARLO GENERATOR

We model the SM background and the effects of ED via the parton-level LO Monte Carlo (MC) generator of Ref. [8], augmented with a parametric simulation of the DØ detector. The simulation takes into account detector acceptance, efficiencies, and resolution, initial state radiation, and the effect of different parton distributions. We used leading order CTEQ4LO [9] distributions to estimate the nominal prediction. The parameters of the detector model are tuned using the $Z(ee)$ data.

The MC includes SM contributions (Z/γ^* and direct diphoton production), Kaluza-Klein graviton exchange diagrams, and their interference in dilepton and diphoton production. Since the parton-level generator involves only the $2 \to 2$ hard-scattering process, we model next-to-leading order (NLO) effects by adding a transverse momentum to the diEM system, based on the measured transverse momentum spectrum of the $Z(ee)$ events.

In the presence of the NLO corrections, the scattering angle θ^* is defined in the diEM helicity frame, i.e., relative to the direction of the boost of the diEM system. Since the parton-level cross section is calculated at LO, we account for NLO effects in the SM background by scaling the cross sections by a constant K-factor of 1.3 [10]. While NLO corrections to the Kaluza-Klein diagrams have not yet been calculated, we use the same constant K-factor for the signal. This choice is reasonable, since the ED diagrams are very similar to those of the SM production.

The K-factor for graviton exchange is expected to grow with invariant mass, similar to that for Z/γ^* exchange [10]; consequently, our assumption tends to underestimate both the ED contribution at high invariant mass (i.e., the signal) and the contribution from the SM (i.e., background) and thus is conservative in terms of sensitivity to the effects of extra dimensions.

We use Bayesian likelihood fitting technique to extract the information on the most likely value of the parameter η_G. The fit uses Monte Carlo templates for double-differential SM cross section, the interference term, and the direct extra dimensional term, and gives an unbiased way of extracting the best estimate of the parameter η_G, as well as to set upper limits on its value. The fit takes into account systematic errors on the signal acceptance and efficiency, K-factor, choice of parton distribution functions, and background estimate.

IV. DATA SELECTION

The data used for this analysis were recorded between April 2002 and November 2003, in the Run II of the Fermilab Tevatron. All the data have been reconstructed with the most modern version of the DØ reconstruction program. These data correspond to a total intergrated luminosity of ≈ 200 pb^{-1} and have been collected via a suit of single EM and diEM triggers, which run unprescaled at all instantaneous luminosities. Given that the analysis is concerned only with high-p_T EM objects, the trigger is $99 \pm 1\%$ efficient for the signal.

We require two EM objects in the event, with the transverse energies above 25 GeV, which pass calorimeter energy isolation, EM energy fraction, calorimeter shower shape, and track isiolation cuts. We reject events that have more than two high-p_T EM objects. The EM clusters are restricted to good fiducial volume of the DØ EM calorimeter: $|\eta_d| < 1.1$ (CC) and $1.5 < |\eta_d| < 2.4$ (EC), where η_d is pseudorapidity, as measured w.r.t. the geometrical center of the DØ detector.

Event kinematics is based on the primary vertex found by standard tracking code. This vertex is then confirmed by means of "EM pointing," i.e., projection of the energy deposits by the EM clusters in the event, which reveal their point of origin. If another vertex is preferred by pointing, we revertex the event accordingly and recalculate all the kinematic parameters. This technique is powerful, since it does not discriminate between diphoton and dielectron events. Studies based on the $Z(ee)$ sample indicate that the hard-scattering vertex is picked in about 96% of the cases. We account for the corresponding 4% misvertexing probability in the fast MC simulation.

The overall efficiency of the EM ID cuts is 0.85 ± 0.01 per electron object in either of the two calorimeters (CC or EC).

Cut	Number of events
Reconstructed Data	∼700 million events
diEM Stream	~ 2 million events
Starting root-tuple sample after duplicate event removal	485K
≥ 2 EM objects w/ $E_T > 20$ GeV and χ^2 cut	39,604
$E_T^{EM} > 25$ GeV, EMF cut, track isolation	18,118 = 9,380 CC-CC + 6,828 CC-EC + 1,910 EC-EC

TABLE I: Event selection.

This selection leaves us with a sample of 18,118 events, as documented in Table I.

Monte Carlo studies of the sensitivity showed that the optimal sensitivity is achieved when the CC-CC and CC-EC topologies are combined in the analysis. Adding the EC-EC topology actually degrades the sensitivity slightly, due to large background in this channel (see next section) and high probability for it to fluctuate. Therefore, we further restrict the analysis to the central-central (CC-CC) and central-forward (CC-EC) topologies.

V. BACKGROUNDS

The SM backgrounds from Drell-Yan production and direct diphoton production are already included in the output of the fast Monte Carlo used to simulate signal. The unaccounted part is instrumental background that comes from dijet and direct photon events, where jet(s) are misidentified as EM objects. An accurate estimate of the misidentification rate requires good understanding of jet energy scale and large statistics, especially at high-E_T, where the signal is expected to dominate SM backgrounds.

The probabality for a jet to "fake" a photon is $\approx 10^{-3}$ in the DØ Run II detector; consequently the contribution from direct-photon events is negligible compared to that from dijets, as the MC studies have shown. Therefore, the instrumental background is dominated by the dijet events, and can be accurately estimated by the technique described below.

We select the events that pass all the selections, except that the EM objects are required to pass anti-quality calorimeter shower shape cuts, orthogonal to the cuts used for the candidate sample.

The resulting sample does not have any appreciable contribution from the signal, as controlled by the lack of the Z-peak seen in it. We use this sample to determine the shape of the misidentification background. We further determine the normalization for this background by fitting the low-mass region of the diEM mass spectrum to the sum of the Drell-Yan and the misidentification background, with the integrated luminosity and the background normalization being free parameters of the fit. Since the effects of large extra dimensions are negligible at low invariant diEM masses, this technique is not biased by a possible presence of the signal in our data.

All other physics backgrounds that results in a diEM final state are negligible.

VI. COMPARISON BETWEEN THE DATA AND BACKGROUNDS

The comparison between the data and predicted background for the base candidate sample with 9,380 CC-CC and 6828 (CC-EC) events is illustrated in Figs. 1 (diEM mass, logarithmic scale), 2 (diEM mass, linear scale) and 3 ($\cos\theta^*$, linear scale).

We observe good agreement between the data and the background in both topologies. To quantify the agreement between the data and the background in the steeply-falling mass spectrum, we calculate the prediction for the background above certain mass cutoff and compare it with the data for a number of mass cutoffs. The results are summarized in Table II.

As the data agrees with the SM predictions, we proceed with setting limits on large extra dimensions.

VII. LIMITS ON LARGE EXTRA DIMENSIONS

The two-dimensional distribution of the diEM mass vs. $\cos\theta^*$ is shown in Fig. 4.

Since the signal and background are very different in the two event topologies, it does not make sense to combine the spectra when extracting limits on extra dimensions. Instead, we extract the limit by constructing likelihood functions for each topology and then properly combining them in the fit.

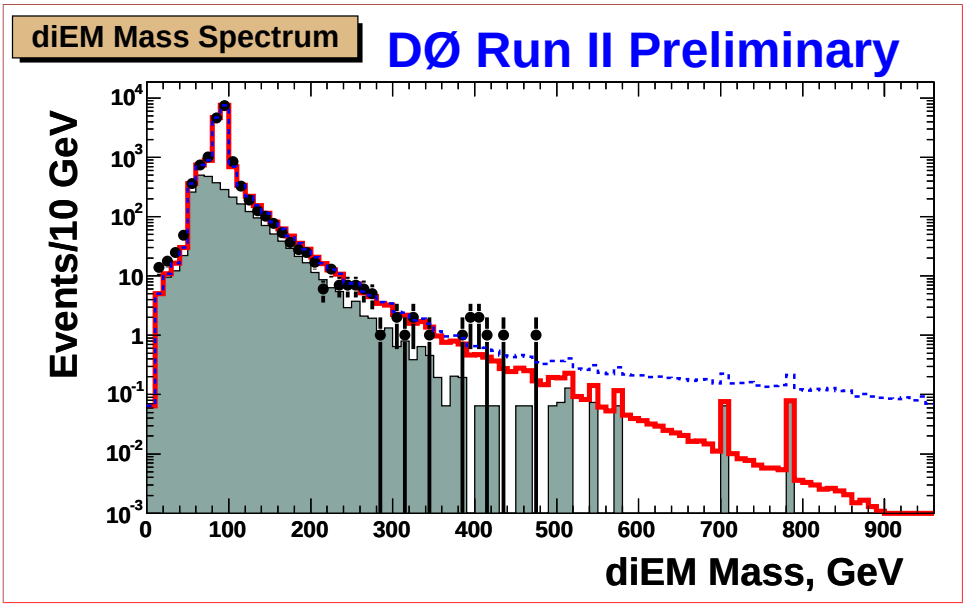

FIG. 1: The diEM mass distribution for the combined CC-CC and CC-EC candidate samples. Points with the error bars are the data; light filled histogram represents the instrumental background from jets misidentified as EM objects; solid line shows the fit to the sum of the instrumental background and the SM predictions from Drell-Yan and direct diphoton backgrounds. The dashed line shows the effect of the ED signal for $\eta_G = 0.6$.

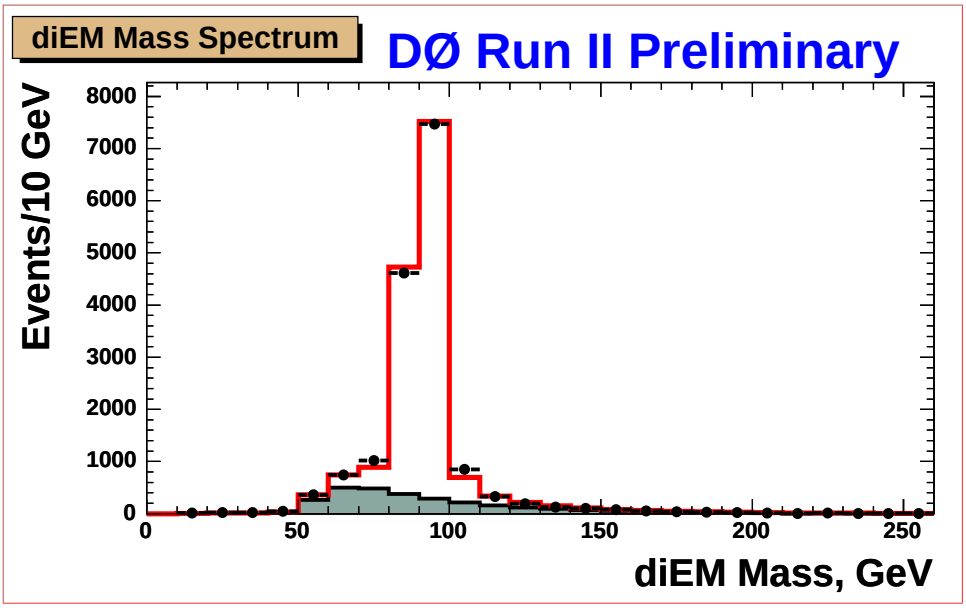

FIG. 2: The diEM mass distribution for the combined CC-CC and CC-EC candidate samples. Points with the error bars are the data; light filled histogram represents the instrumental background from jets misidentified as EM objects; solid line shows the fit to the sum of the instrumental background and the SM predictions from Drell-Yan and direct diphoton backgrounds.

When setting limits on extra dimensions, we assign systematic uncertainties of 15% on signal and 7-20% on background estimates, as documented in Table III. The uncertainty on the signal is dominated by the uncertainty on the shape of the NLO corrections (i.e., energy dependence of the K-factor, 10%), possible residual E_T-dependence of the efficiency (5%), and uncertainty due to the choice of parton distribution functions. The 20% uncertainty in the background is due to the statistics and systematics of the instrumental background. The latter dominates only at high diEM masses, most sensitive to the effects of extra dimensions, and this is where the quoted uncertainty applies. At lower masses, the uncertainty on the background is dominated by the uncertainty on the product of integrated

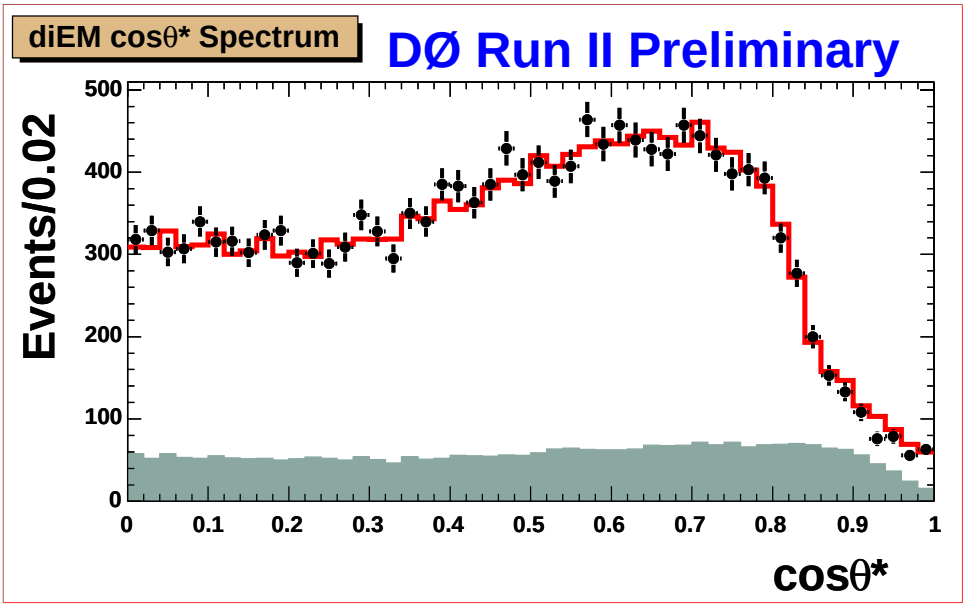

FIG. 3: The diEM $\cos\theta^*$ distribution for the combined CC-CC and CC-EC candidate samples. Points with the error bars are the data; light filled histogram represents the instrumental background from jets misidentified as EM objects; solid line shows the fit to the sum of the instrumental background and the SM predictions from Drell-Yan and direct diphoton backgrounds.

Minimum $M_{\mathrm{EM-EM}}$	Bck, CC-CC	N Events, CC-CC	BCK, CC-EC	N Events, CC-EC	BCK, overall	QCD bck.	Data
50 GeV	9254	9300	6851	6802	16106	2823	16102
100 GeV	775	833	1129	1067	1904	893	1900
150 GeV	120	119	249	185	368	212	304
200 GeV	41.6	41	68.1	42	110	51	83
250 GeV	17.7	19	23.7	14	41.3	15	33
300 GeV	8.2	10	9.1	4	17.3	4.6	14
350 GeV	4.5	6	3.6	2	8.1	1.6	8
400 GeV	2.6	4	1.8	1	4.4	0.9	5
450 GeV	1.6	1	1.0	0	2.6	0.7	1
480 GeV	1.2	0	0.69	0	1.9	0.6	0

TABLE II: Comparison between the data and expected background for events above certain diEM mass cutoffs. Middle two columns show the number of candidate events and predicted background above the diEM mass listed in the first column. Note an additional systematic error of 7–20% on the background prediction, depending on the mass.

luminosity, selection efficiency, and the K-factor, which amounts to 7%.

Source of systematics	Uncertainty
K-factor	10%
Choice of p.d.f.	5%
Luminosity times efficiency	2%
E_T dependence of the efficiency	5%
Total	12%

TABLE III: Sources of systematic uncertainty on the calculated differential cross section.

We then proceed with extracting the best estimate for parameter η_G by fitting the two-dimensional distributions to the sum of the SM, interference, and the direct gravity templates. We first perform the fit separately for both topologies. The size of the 2D-grid used in the main analysis in $M \times \cos\theta^*$ is 50×10. The results are stable w.r.t.

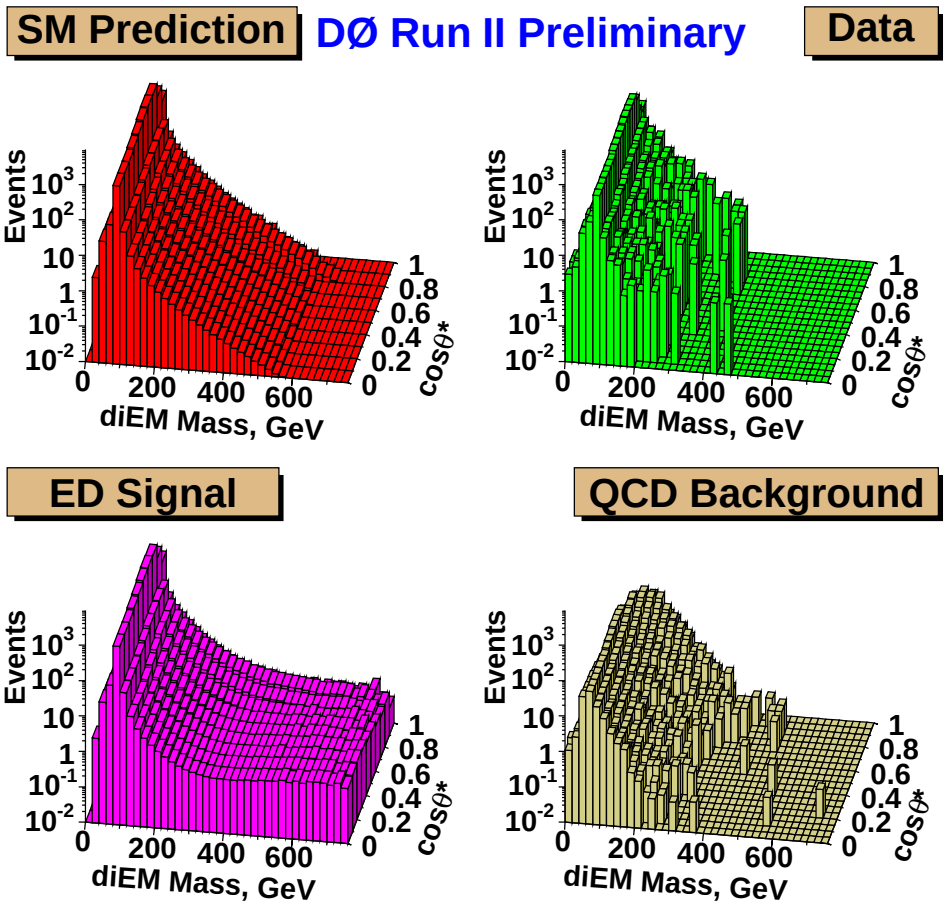

FIG. 4: The diEM mass vs. $\cos\theta^*$ distribution for the base CC-CC and CC-EC candidate sample. Top left: SM background from Drell-Yan and direct diphotons; top right: data; bottom left: ED signal plus the SM background for $\eta_G = 2.0$; bottom right: instrumental background.

the granularity of the grid. The best estimate on the parameter η_G from the fits are:

$$\eta_G = 0.00\ ^{+0.16}_{-0.00}\ \text{TeV}^{-4}\ \text{(CC-CC)};$$
$$\eta_G = 0.00\ ^{+0.26}_{-0.00}\ \text{TeV}^{-4}\ \text{(CC-EC)}; \quad (5)$$
$$(6)$$

i.e. consistent with zero (no gravity contribution), as expected. The 95% upper CL limit on η_G is determined to be:

$$\eta_G^{95\%}\text{(CC-CC)} = 0.341\ \text{TeV}^{-4};$$
$$\eta_G^{95\%}\text{(CC-EC)} = 0.820\ \text{TeV}^{-4} \quad (7)$$

Note that the limits obtained in the CC-CC channel alone are already better than the Run I limit [2] ($\eta_G = 0.46$ TeV^{-4}), obtained with the full detector coverage. The main reasons for that is the increased c.o.m. energy of the upgraded Tevatron and having nearly twice the data of Run I.

We then combine both the CC-CC and CC-EC fits via combining the individual likelihoods and taking into account common systematics. The combined fit yields:

$$\eta_G = 0.00\ ^{+0.115}_{-0.00}\ \text{TeV}^{-4}; \quad (8)$$

$$\eta_G^{95\%} = 0.292\ \text{TeV}^{-4}. \quad (9)$$

The obtained limit agrees well with the expected sensitivity of the combined CC-CC and CC-EC samples, see Fig. 5. The limits are numerically very close to those obtained using a frquentist Poisson likelihood fit.

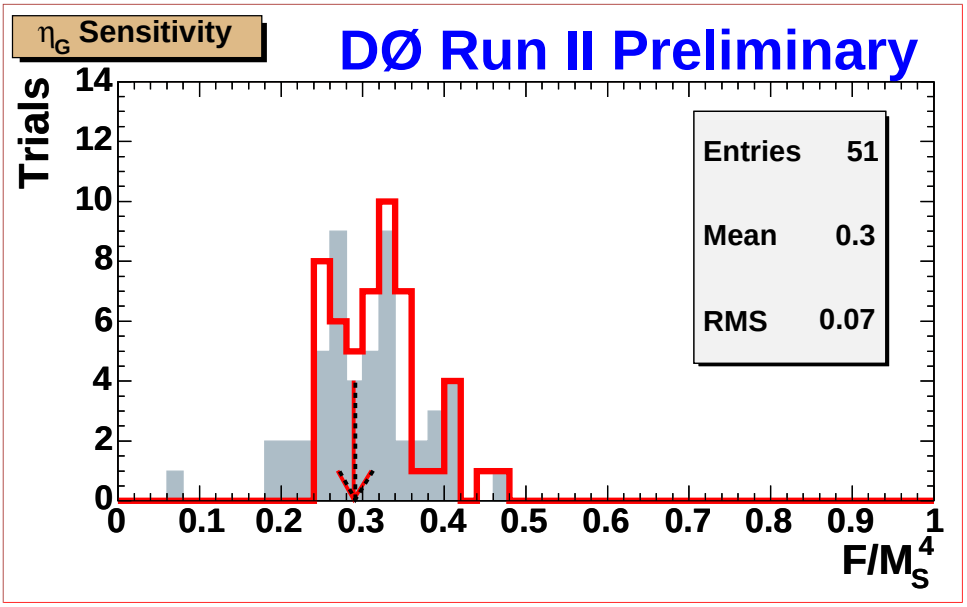

FIG. 5: Expected 95% CL upper limit on the parameter η_G from an ensemble of MC experiments, together with the actual limits obtained in this analysis. Shaded histogram: Bayesian limit; open histogram: Likelihood limit. The arrows indicate Bayesian (solid) and Likelihood (dashed) limits derived from data. Both the CC-CC and CC-EC combinations are used for the ensemble tests and for the limit from data.

We also obtain limits for negative sign of the interference term, possible in Hewett's convention. The procedure is the same, and the corresponding results are: The combined fit yields:

$$\eta_G = -0.08 \ {}^{+\,0.08}_{-\,0.18} \ \text{TeV}^{-4}; \tag{10}$$

$$\eta_G^{95\%} = -0.432 \ \text{TeV}^{-4}. \tag{11}$$

We translate limits on η_G into limits on the fundamental Planck scale, M_S. The results are summarized in Table IV. For the HLZ formalism, $n = 2$, we used average value of M^2 at the Tevatron, which is $(0.66 \text{ TeV})^2$ [8]. These limits are the tightest limits on large extra dimensions from a single measurement.

GRW [4]	HLZ [5]						Hewett [6]
	n=2	n=3	n=4	n=5	n=6	n=7	$\lambda = +1/\lambda = -1$
1.36	1.56	1.61	1.36	1.23	1.14	1.08	1.22/1.10

TABLE IV: Lower limits at 95% CL on the fundamental Planck scale, M_S, in TeV.

VIII. COMBINATION WITH RUN I RESULT

We further combine this result with the published Run I limit [2] via the likelihood combination method. Since the Run II apparatus is largely different from that in Run I, and since the collision energy is different as well, the only common source of systematics is the K-factor used for signal and SM cross sections. To combine the two measurements with this common source of systematics, we take the Bayesian likelihood from the Run I analysis and multiply it by the Bayesian likelihood of the Run II analysis with the uncertainty on the K-factor set to 0. (The last step, although technically correct, is largely redundant, as the systematic error on the K-factor is effectively bound in the fit procedure by the normalization to the Z-peak and does not affect the results of the fit by much.)

The normalized Run I, II, and combined likelihood functions are shown in Fig. 6. The combined 95% CL limit on parameter η is 0.24 TeV^{-4}, which can be translated into the limits on the fundamental Planck scale M_S, as shown in Table V. These limits are the most stringent limits on large extra dimensions to date.

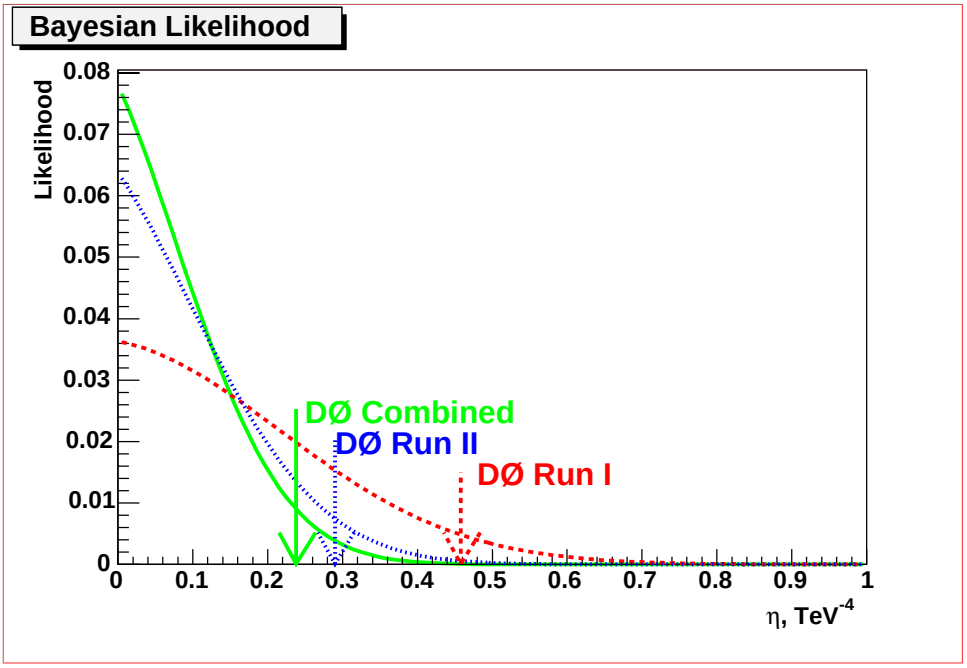

FIG. 6: Bayesian likelihood for the Run I (dashed), Run II (dotted), and combined analyses. Arrows indicate 95% CL limits on parameter η.

GRW [4]	HLZ [5]						Hewett [6]
	n=2	n=3	n=4	n=5	n=6	n=7	$\lambda = +1$
1.43	1.67	1.70	1.43	1.29	1.20	1.14	1.28

TABLE V: Combined lower limits at 95% CL on the fundamental Planck scale, M_S, in TeV.

IX. INTERESTING CANDIDATE EVENTS

One feature that stands out in the diEM invariant mass plot are eight candidate events with mass above 350 GeV. Six of these events form a bump at 400 GeV. We took a closer look at these events and they do not appear to come from a single resonance for the following reasons:

- All but two of the events in the peak have only one or zero tracks matched with the EM objects. Given $\approx 80\%$ tracking efficiency in the central region, that disfavors a possibility for these events to originate from a resonance decaying into dielectrons, e.g. Z';
- The number of candidate events scales up and down with the change of EM ID cuts with the rate typical of a QCD background rather than with the rate expected due to the losses in efficiency. Particularly, removing the tracking isolation cut increases the number of candidates by 5, with only 12% increase in efficiency;
- The bump is about twice as narrow as expected from a narrow resonance smeared with the typical DØ EM calorimeter resolution.

We conclude that the above evidence does not support a hypothesis that these events come from a new resonance. Most of them have large values of $\cos\theta^*$ making them characteristic of diphoton/QCD background events.

The two candidate events with the highest mass are more interesting. Their parameters are listed in Table VI. The event displays of these two events are shown in Figs. 7, 8, and Figs. 9, 10.

Run	Event	$\not\!\!E_T$	Type	E_T^1 (p_T^1)	E_T^2 (p_T^2)	η_1	η_2	ϕ_1	ϕ_2	M	$\cos\theta^*$	$N_{\rm jet}$
177851	28783974	8.8	e^+/e^-	239.2 (190.8)	226.9 (234.4)	-0.45	-0.50	0.48	3.68	475	0.01	1
175826	15382214	17.0	$\gamma\gamma$	197.9	158.4	-0.47	0.87	3.20	0.06	436	0.03	0

TABLE VI: Parameters of the two highest diEM mass candidates. Both events have only one reconstructed vertex, in a good agreement with the vertex from EM pointing. All energy variables are in GeV.

While the pure count of events at high masses agrees well with the SM predictions, the two highest mass events both have very low value of $\cos\theta^*$, essentially equal to zero. While the SM events are expected to be distributed uniformly in $\cos\theta^*$, signal events are accumulated at low value of $\cos\theta^*$. (This would also be true for a signal in certain compositeness models.) Another interesting observation is that one event is a perfectly measured e^+e^- pair, while the other one is a diphoton event.

Clearly, it's too early to draw any conclusions from the observed candidates, except that the DØ detector is working well and is capable of detecting very clean high-mass diphotons and dileptons. These events, though intriguing, are consistent with the SM. We will search with interest for similar events as additional data are recorded.

X. CONCLUSIONS

We performed search for large extra spatial dimensions using ~ 200 pb^{-1} of data collected by the DØ experiment in Run II of the Fermilab Tevatron. The lower 95% CL limit on the fundamental Planck scale was set to be 1.36 TeV in the GRW convention. Combined with our previously published Run I measurement [2], it results in even more stringent limit of 1.43 TeV, which is the tightest limit on large extra dimensions to date.

While data agree with the SM, we see two interesting candidate events, one in the dielectron, and one in the diphoton channel, whose properties (very high mass and scattering angle very close to $\pi/2$) would make them excellent candidates for new physics beyond the SM, e.g. Large Extra Dimensions. The increased statistics of Run II will provide the definitive answer whether these events are coming from the SM processes or indicate new physics beyond the Standard Model.

Acknowledgments

We thank the staffs at Fermilab and collaborating institutions, and acknowledge support from the Department of Energy and National Science Foundation (USA), Commissariat à L'Energie Atomique and CNRS/Institut National de Physique Nucléaire et de Physique des Particules (France), Ministry for Science and Technology and Ministry for Atomic Energy (Russia), CAPES, CNPq and FAPERJ (Brazil), Departments of Atomic Energy and Science and Education (India), Colciencias (Colombia), CONACyT (Mexico), Ministry of Education and KOSEF (Korea), CONICET and UBACyT (Argentina), The Foundation for Fundamental Research on Matter (The Netherlands), PPARC (United Kingdom), Ministry of Education (Czech Republic), A.P. Sloan Foundation, Civilian Research and Development Foundation, Research Corporation, Texas Advanced Research Program, and the Alexander von Humboldt Foundation.

[1] N. Arkani-Hamed, S. Dimopoulos, G. Dvali, Phys. Lett. **B429**, 263 (1998); I. Antoniadis, N. Arkani-Hamed, S. Dimopoulos, and G. Dvali, Phys. Lett. **B436**, 257 (1998); N. Arkani-Hamed, S. Dimopoulos, G. Dvali, Phys. Rev. D **59**, 086004 (1999); N. Arkani-Hamed, S. Dimopoulos, J. March-Russell, SLAC-PUB-7949, e-Print Archive: hep-th/9809124.
[2] B. Abbott *et al.* (DØ Collaboration), Phys. Rev. Lett. **86**, 1156 (2001).
[3] V. Abazov *et al.* (DØ Collaboration), Phys. Rev. Lett. **90**, 251802 (2003).
[4] G. Giudice, R. Rattazzi, and J. Wells, Nucl. Phys. **B544**, 3 (1999), and revised version hep-ph/9811291.
[5] T. Han, J. Lykken, and R. Zhang, Phys. Rev. D **59**, 105006 (1999), and revised version hep-ph/9811350.
[6] J. Hewett, Phys. Rev. Lett. **82**, 4765 (1999).
[7] A. Gupta, N. Mondal, and S. Raychaudhuri, TIFR-HECR-99-02, hep-ph/9904234; K. Cheung, hep-ph/9904266.
[8] K. Cheung and G. Landsberg, Phys. Rev. D **62**, 076003 (2000).
[9] H.L. Lai *et al.*, Phys. Rev. **D51**, 4763 (1995).
[10] R. Harnberg, W.L. Van Neerven, and T. Matsura, Nucl. Phys. B**359**, 343 (1991); S. Mrenna, private communication.

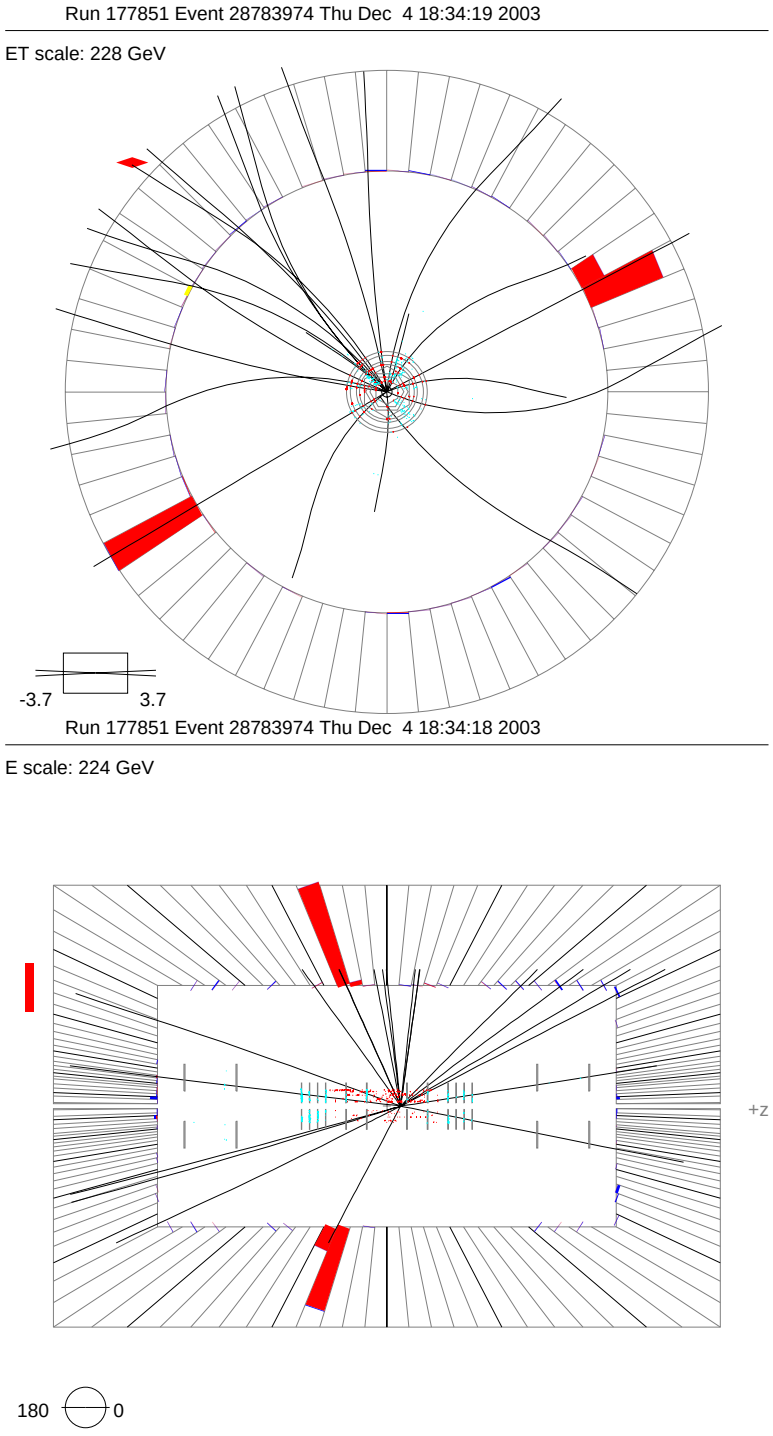

FIG. 7: Event display of the highest-mass diEM candidate with the invariant mass of 475 GeV and $\cos\theta^*$ of 0.01 (Run 177851, Event 28783974, or "Event Callas"). The event is the highest mass Drell-Yan candidate ever observed. It also possesses kinematics typical of a signal from large ED. The event parameters have been largely overconstrained by multiple DØ subdetectors.

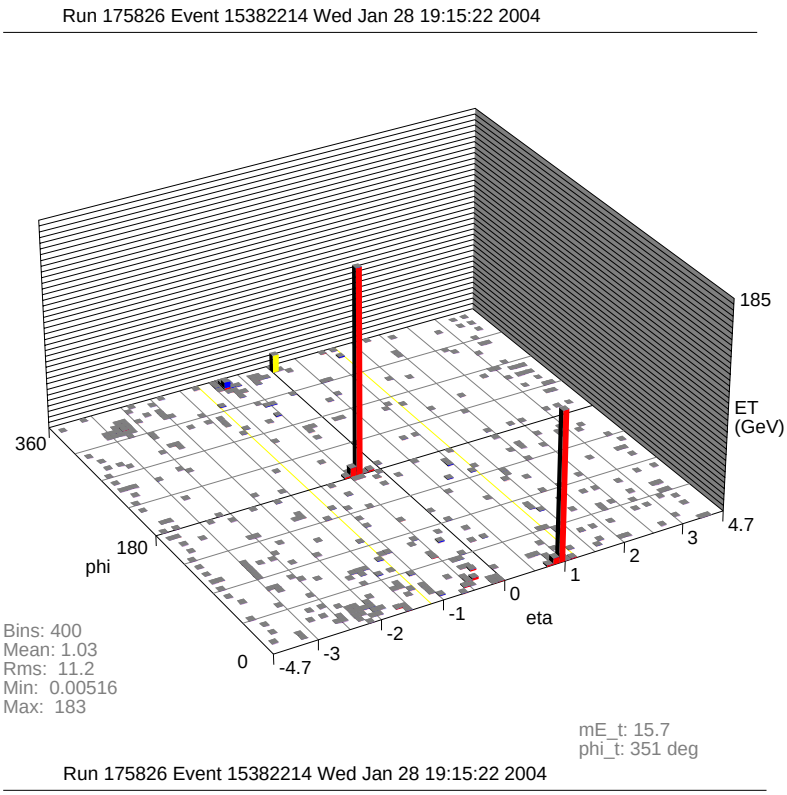

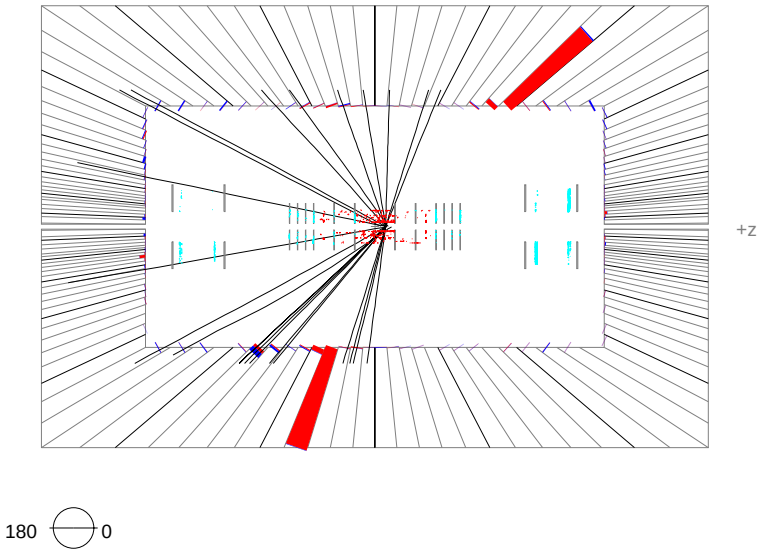

FIG. 8: Event display of the second-highest-mass diEM candidate with the invariant mass of 435 GeV and $\cos\theta^*$ of 0.02 (Run 169736, Event 23391029). Event display of the highest-mass diEM candidate with the invariant mass of 476 GeV and $\cos\theta^*$ of 0.01 (Run 175826, Event 15382214). The event is the highest mass diphoton candidate ever observed. It also possesses kinematics typical of a signal from large ED.

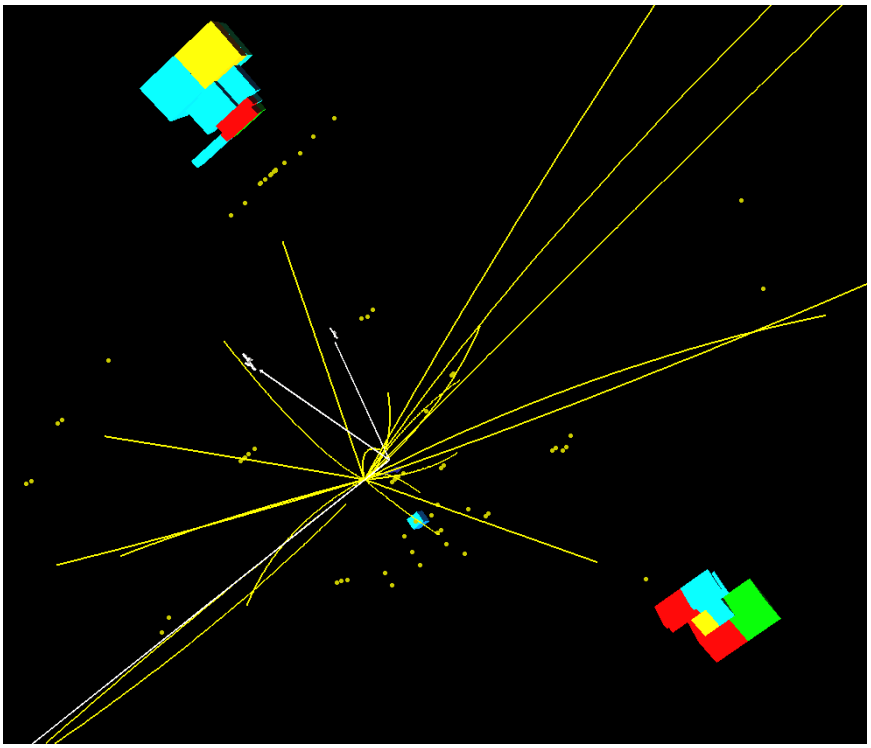

FIG. 9: 3D-view of event Callas.

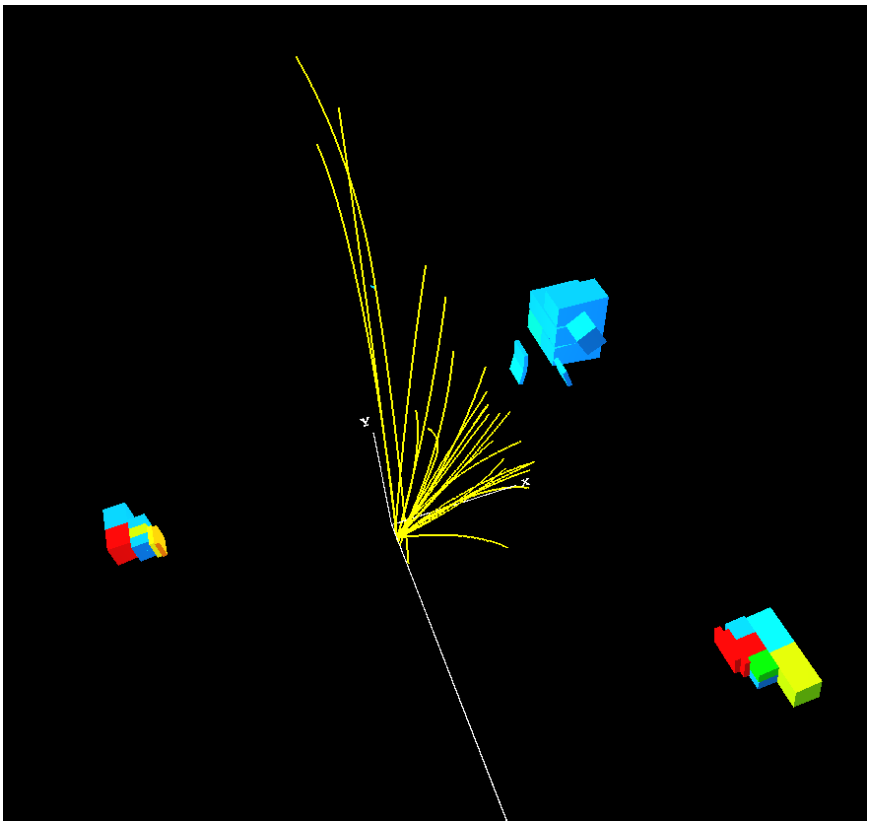

FIG. 10: 3D-view of the second-highest-mass event.